RESEARCH ARTICLE

Macromolecular Chemistry and Physics
www.mcp-journal.de

Cationic Fluorinated Polyphosphazenes for Efficient Decontamination of Anionic Pollutants from Wastewater

Francesco Lanero, Marina Ramos-Martín, Keti Vezzù, Vito Di Noto, Joaquín García-Álvarez, Alessandro Scarso, Paolo Sgarbossa,* and Alejandro Presa Soto**

This work presents a simple and efficient methodology for the synthesis of well-defined fluorinated copolyphosphazenes incorporating 2,2,2-trifluoroethan-1-olate (–OCH_2CF_3, TFE) and 3-(diethylamino)phenolate (3DEAP) side groups, randomly distributed along the polymer chains, via living cationic polymerization. Two fluorinated copolyphosphazenes, 4a and 4b, with different CF_3/3DEAP ratios (1:1 and 1:3, respectively), are prepared. The 3DEAP groups in these polymers are selectively and smoothly quaternized using methyl iodide (CH_3I), yielding cationic fluorinated copolyphosphazenes 5a and 5b with quaternization degrees of ≈80% and 90%, respectively. These cationic copolymers, featuring tailored CF_3/3DEMAP$^+$ ratios (3DEMAP$^+$ = 3-(diethyl(methyl)ammonio)phenolate), exhibit complete water solubility and demonstrate self-assembly in aqueous solutions, forming large compound micelles (LCMs) or bilayer vesicles depending on their composition. The amphiphilic nature of these materials, combining hydrophobic (CF_3) and hydrophilic (3DEMAP$^+$) moieties, enables their application in the efficient capture of anionic pollutants, such as sodium diclofenac (SDF) and perfluorooctanoic acid (PFOA), commonly found in wastewater. This study highlights the potential of these cationic fluorinated copolyphosphazenes as promising candidates for water decontamination and environmental remediation.

1. Introduction

In recent years, synthetic polymer materials have gained significant attention in several research fields, like drug delivery research and water purification.[1,2] Unlike natural polymers, synthetic polymers offer greater flexibility in structural design, allowing for the creation of systems tailored to specific needs. Among these, fluoropolymers are highly specialized materials with exceptional properties, including thermal stability, chemical resistance (to solvents, acids, bases, and water), low water absorption, low refractive indices, and excellent durability and oxidation resistance.[3–5] These characteristics make them critical for high-tech applications, such as elastomers, protective coatings, fuel cell membranes, automotive components (seals, gaskets, cables, and lithium–ion battery membranes), aerospace (fire-retardant coatings, cables, and O-rings), microelectronics, chemical engineering (high-performance membranes), and optics (optical fibers).[6–10] Their versatility and performance establish them as essential materials in advanced industries. Despite their remarkable properties, fluoropolymers face significant limitations. Homopolymers often exhibit high crystallinity, leading to poor solubility in common organic solvents. To address these challenges, fluorinated copolymers have been developed, often incorporating ionic functionalities that disrupt the crystalline structure of homopolymers, thereby enhancing solubility, processability, and applicability.[3,9,11] In this context, the development of synthetic strategies to prepare ionic fluorinated copolymers—enabling "*on-demand*" control over functional group density and tailored properties while maintaining excellent chemical stability—remains a growing area of interest.

Polyphosphazenes (PPz), hybrid polymers featuring an inorganic backbone of alternating phosphorus and nitrogen atoms (—P=N—) and organic side groups, emerge as highly promising materials due to their structural versatility and controllable chain degradation. These synthetic macromolecules are unique, combining unprecedented backbone flexibility with straightforward main-chain functionalization through diverse organic substituents.[12–17] By precisely balancing hydrophilic and hydrophobic properties, these materials can be engineered for specific applications.[18–28] In this regard, while the chemistry

F. Lanero, K. Vezzù, V. Di Noto, P. Sgarbossa
Department of Industrial Engineering
University of Padova
via Marzolo 9, Padova 35131, Italy
E-mail: paolo.sgarbossa@unipd.it
M. Ramos-Martín, J. García-Álvarez, A. Presa Soto
Department of Organic and Inorganic Chemistry (IUQOEM)
University of Oviedo
Av. Julián Clavería 8, Oviedo 33006, Spain
E-mail: presaalejandro@uniovi.es
A. Scarso
Department of Molecular Science and Nanosystems
Ca' Foscari University of Venice
Via Torino 155, Mestre, Venezia 30172, Italy
E-mail: alesca@unive.it

The ORCID identification number(s) for the author(s) of this article can be found under https://doi.org/10.1002/macp.202500154

DOI: 10.1002/macp.202500154

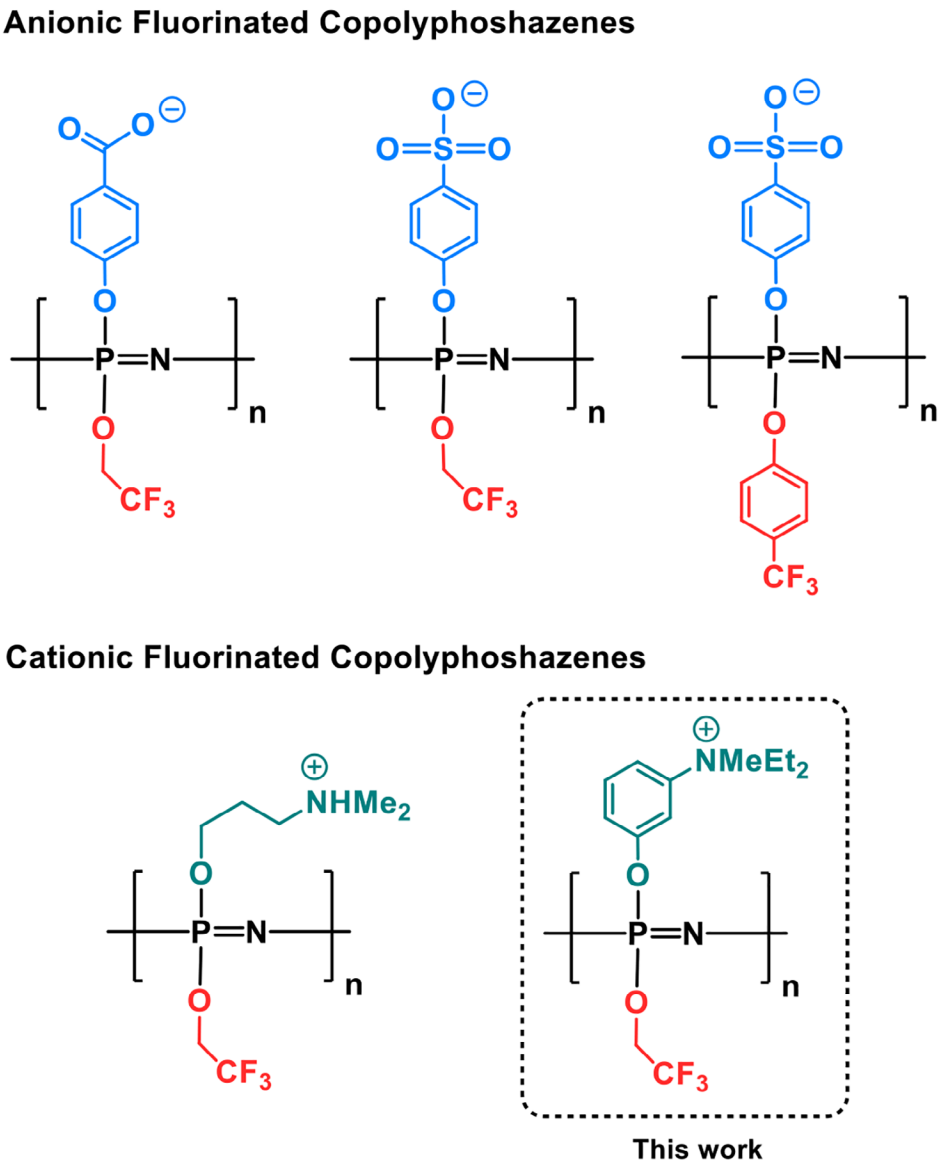

Figure 1. Schematic examples of the reported structures of anionic and cationic fluorinated copolyphosphazenes.

of fluorophosphazenes has been extensively studied for high-performance elastomers, membranes, and surface coatings,[29,30] the chemistry of ionic fluorinated polyphosphazenes remains significantly less explored. Thus, Andrianov et al. described the synthesis of polyphosphazene polyelectrolytes containing hydrophobic fluorinated moieties, such as 2,2,2-trifluoroethan-1-olate (–OCH_2CF_3, TFE) and/or 4-(trifluoromethyl)phenolate (-$OC_6H_4CF_3$, TFMP) side groups, along with variable amounts of anionic sulfonate[31] or carboxylate[32–34] substituents (**Figure 1**). These water-soluble anionic fluorinated copolyphosphazene demonstrated promising performance as coatings on various biomedically relevant planar and porous substrates, exhibiting selective protein adsorption, exceptionally low hemolysis, and antibacterial activity.[31–33] Subsequently, the same research group described the synthesis of a cationic fluorinated counterpart incorporating TFE side groups (–OCH_2CF_3) and cationic dimethylammonium moieties (Figure 1).[35] These materials spontaneously formed stable supramolecular complexes with heparin and served as hemocompatible nanocoatings. Motivated by the challenges in synthesizing cationic fluoropolymers with "*on-demand*" fluorine content and controlled solubility in aqueous media—and to the best of our knowledge, this being the only example of a polyphosphazene with such characteristics reported to date—we herein present an efficient synthetic pathway to develop novel cationic fluorinated random copolyphosphazenes. These materials feature a well-controlled molecular weight distribution and tailored fluorinated/cationic side-group ratios, making them highly effective as decontamination agents for anionic pollutants in wastewater.

The increasing consumption of pharmaceuticals and personal care products has raised significant environmental concerns, as these compounds often persist in water bodies

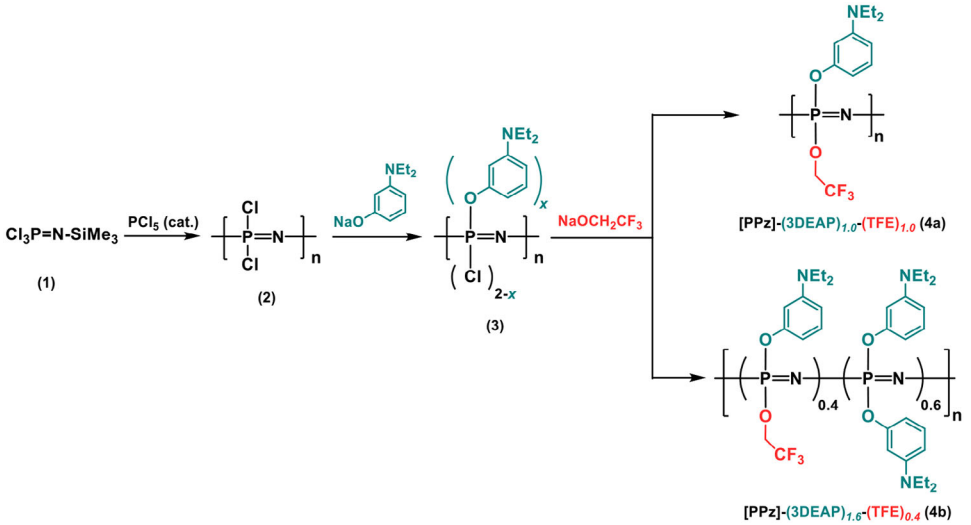

Scheme 1. General synthetic pathway for non-ionic fluorinated copolyphosphazenes [PPz]-(3DEAP)$_{1.6}$-(TFE)$_{0.4}$ (**4a**) and [PPz]-(3DEAP)$_{1.0}$-(TFE)$_{1.0}$ (**4b**) exhibiting different TFE/3DEAP ratios.

and disrupt ecosystems.[36] Similarly, per- and polyfluoroalkyl substances (PFASs), widely used since the 1950s in industrial and commercial applications, pose a major challenge due to their extreme chemical and thermal stability, leading to long-term environmental persistence and widespread detection in water, wildlife, and humans.[37] Among these contaminants, sodium diclofenac (SDF), a nonsteroidal anti-inflammatory drug with an annual global consumption of 2400 tons,[38] is particularly concerning due to its nonbiodegradability, high polarity, and water solubility, which hinder its removal in conventional water treatment systems.[39] Likewise, perfluorooctanoic acid (PFOA), extensively used in surfactants, fire retardants, and fluoropolymer production, has become ubiquitous in water sources, including drinking water.[40] Both SDF and PFOA are linked to toxicity and potential carcinogenic effects, underscoring the urgent need for effective remediation strategies. While methods such as adsorption,[41] oxidative degradation,[42,43] and photocatalysis[44] have been explored for SDF removal, PFOA elimination often relies on techniques like electrochemical oxidation,[45] UV/sulfite treatment,[46] biological processes,[47,48] and photocatalysis.[49] These challenges highlight the critical demand for innovative solutions to address their environmental and health impacts.

In this work, we present a flexible synthetic route to obtain well-defined copolyphosphazenes featuring both hydrophilic tertiary amino groups (3-(diethylamino)phenolate, 3DEAP) and hydrophobic fluorinated moieties (TFE side groups), allowing for precise tuning of the water solubility of the final polymer. Through selective quaternization of the amino groups, novel cationic fluorinated random copolyphosphazenes with tailored CF_3/3DEMAP$^+$ ratios were synthesized (Figure 1). These materials exhibited water solubility and demonstrated the ability to self-assemble in aqueous solutions, forming large compound micelles (LCMs) or bilayer vesicles depending on their CF_3/3DEMAP$^+$ ratio. Furthermore, the capacity of these cationic fluorophosphazenes to bind anionic pollutants, such as sodium diclofenac (SDF) and perfluorooctanoic acid (PFOA), was investigated. NMR experiments revealed the formation of stable insoluble complexes, highlighting the potential of these materials for the effective sequestration of both pharmaceutical and perfluorinated substances in their anionic forms.

2. Results and Discussion

2.1. Synthesis and Characterization of Non-Ionic Fluorinated Copolyphosphazenes

The synthesis of non-ionic fluorinated copolyphosphazenes [PPz]-(3DEAP)$_x$-(TFE)$_{2-x}$ (3DEAP = 3-(diethylamino)phenolate; TFE = 2,2,2-trifluoroethan-1-olate), **4a** (x = 1.0) and **4b** (x = 1.6), was carried out through a sequential macromolecular nucleophilic substitution of poly(dichloro)phosphazene (**2**). This involved the reaction with varying amounts of sodium 3-(diethylamino)phenolate, followed by treatment with an excess of sodium 2,2,2-trifluoroethan-1-olate (see **Scheme 1** and Experimental Section for detailed experimental procedures). Initially, the cationic living polymerization of trichlorophosphoranimine (**1**), promoted by PCl_5, yielded monodisperse poly(dichloro)phosphazene (**2**) chains.[50–52] The number of repeating units (200 for [PPz]-(3DEAP)$_{1.6}$-(TFE)$_{0.4}$ (**4a**) and 175 for [PPz]-(3DEAP)$_{1.0}$-(TFE)$_{1.0}$ (**4b**)) was determined based on the relative integration of the signals corresponding to the -PCl_3^+ end groups (≈8 ppm) and the —N=PCl_2— units (≈−18 ppm) in the ^{31}P-NMR spectrum of the crude product. Subsequently, the chlorine atoms were replaced through sequential treatment of the obtained poly(dichloro)phosphazene (**2**) with varying molar ratios of sodium 3-(diethylamino)phenolate and sodium 2,2,2-trifluoroethan-1-olate, respectively. This led to the formation of the fluorinated polyphosphazenes [PPz]-(3DEAP)$_{1.0}$-(TFE)$_{1.0}$ (**4a**) and [PPz]-(3DEAP)$_{1.6}$-(TFE)$_{0.4}$ (**4b**) in good yields (83% and 79%, respectively), with variable proportions of hydrophobic fluorinated TFE groups randomly distributed along the polymeric chains.

The ^{31}P-NMR spectra of both polymers confirm the efficient nucleophilic macromolecular substitution of the chlorine atoms

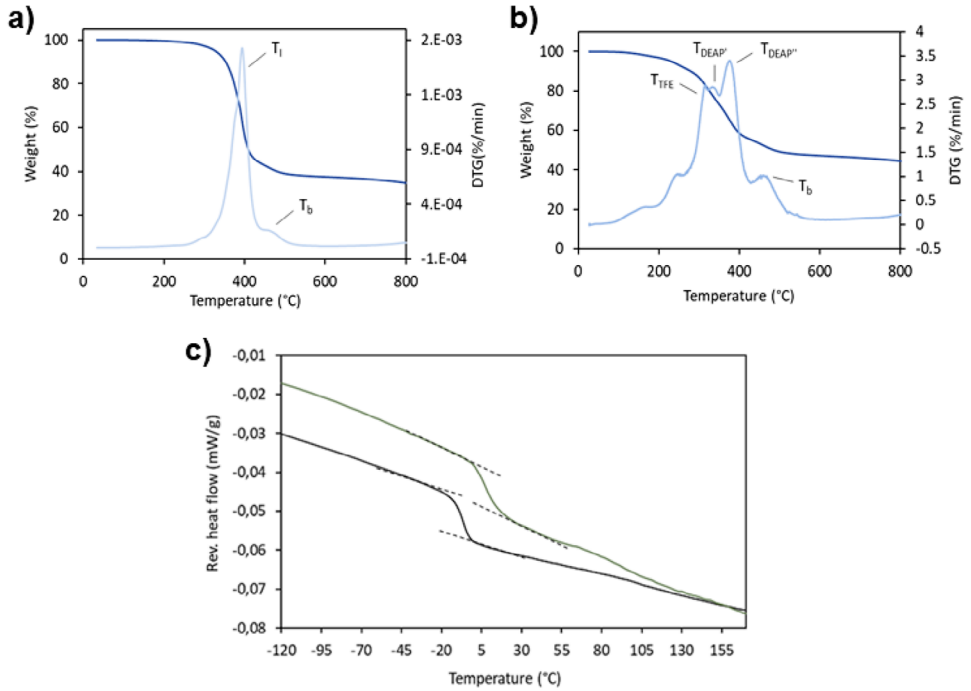

Figure 2. TGA (dark blue) and DTG (light blue) curves of non-ionic fluorinated copolyphosphazenes: a) **4a** ([PPz]-$(3DEAP)_{1.0}$-$(TFE)_{1.0}$) and b) **4b** ([PPz]-$(3DEAP)_{1.6}$-$(TFE)_{0.4}$). c) DSC thermograms of non-ionic fluorinated copolyphosphazenes **4a** (black) and **4b** (green).

in poly(dichloro)phosphazene (**2**) (Figures S1 and S2, Supporting Information), as well as the presence of cyclo- and oligophosphazenes generated during the chlorine replacement reaction (less than 1.0 mol%, based on relative integration). The 3DEAP/TFE ratios of copolyphosphazenes **4a** and **4b** were determined by relative integration of the signals corresponding to both substituents in the ^{1}H-NMR spectra (Figures S3 and S4, Supporting Information). The ATR-FTIR spectra (Figures S5 and S6, Supporting Information) of copolyphosphazenes **4a** and **4b** displayed, in addition to the characteristic bands of the phosphorus-nitrogen backbone stretching (1167 and 1268 cm^{-1}), bands associated with the C—F (960 cm^{-1}) and C—N (1242 cm^{-1}) stretching modes. The latter band is particularly relevant as it also confirms the quaternization of the 3DEAP groups (discussed later). The use of living cationic polymerization for the synthesis of poly(dichloro)phosphazene (**2**) enabled precise control over the molecular weights of the fluorinated copolymers **4a** (M_n = 80 200 Da) and **4b** (M_n = 85 500 Da), resulting in very low polydispersity indices ($Đ$ = 1.19 and 1.21, respectively; Figure S7, Supporting Information).

The thermal stability of the as-prepared copolyphosphazenes **4a** and **4b** was evaluated by TGA/DTG (**Figure** 2a,b). The DTG curve of the fluorinated copolyphosphazene **4a** (Figure 2a) revealed two main degradation events at temperatures of T_I = 400 °C and T_b = 460 °C. The first event (T_I) corresponds to the degradation of the pendant groups, while the second (T_b) is attributed to the breakdown of the polyphosphazene backbone via the formation of cyclic and linear oligomers.[53] In contrast, copolyphosphazene **4b**, with a higher 3DEAP content, exhibited a significantly different decomposition pattern, where the degradation of each side group (TFE and 3DEAP) could be clearly distinguished (Figure 2b). Specifically, the loss of TFE groups was observed at 315 °C (T_{TFE}), while the degradation of the 3DEAP groups occurred at higher temperatures, with the loss of NEt_2 groups at 335 °C ($T_{DEAP'}$) and the aromatic rings at 380 °C ($T_{DEAP''}$).[54] Finally, the degradation of the polymer backbone (T_b) took place at the same temperature as that of copolyphosphazene **4a** (460 °C).

The DSC thermograms of the fluorinated copolyphosphazenes **4a** and **4b** both exhibit an endothermic shift in heat capacity associated with a glass transition (T_g) between −10 and 10 °C (Figure 2c). As expected, the presence of the bulky 3DEAP side group leads to a significant increase in the T_g values of both copolymers compared to that of the homopolymer $[N{=}(OCH_2CF_3)_2]_n$, which has a T_g of −60 °C.[55] Consistently, the higher 3DEAP/TFE ratio in copolymer **4b** compared to **4a** results in an increase in the T_g of the former (10 °C) relative to the latter (−6 °C).[56]

2.2. Synthesis and Characterization of Cationic Fluorinated Copolyphosphazenes

The quaternization of 3DEAP side groups of copolyphosphazenes **4a** and **4b** was studied using CH_3I as the methylation agent under varying experimental conditions (solvent, temperature, and time). It was found that the best yields and degrees of methylation for copolymers **4a** and **4b** were achieved using a temperature of 55 °C, a solvent mixture of $CHCl_3/CH_3CN$ (1:3), and a reaction time of 18 h (**Scheme** 2). This approach yielded the cationic fluorinated copolyphosphazenes [PPz]-$[(3DEAP)_{0.1}(3DEMAP^+)_{0.9}]$-

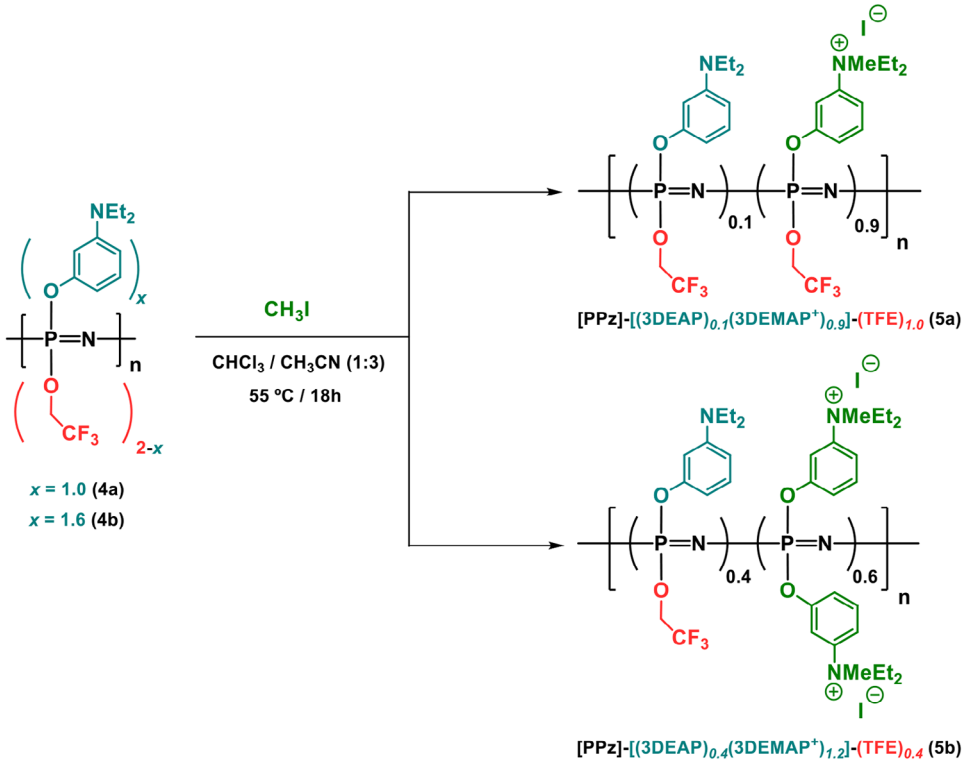

Scheme 2. General synthetic pathway for cationic fluorinated copolyphosphazenes [PPz]-[(3DEAP)$_{0.1}$(3DEMAP$^+$)$_{0.9}$]-(TFE)$_{1.0}$ (**5a**) and [PPz]-[(3DEAP)$_{0.4}$(3DEMAP$^+$)$_{1.2}$]-(TFE)$_{0.4}$) (**5b**) exhibiting different quaternization ratios.

(TFE)$_{1.0}$ (**5a**) and [PPz]-[(3DEAP)$_{0.4}$(3DEMAP$^+$)$_{1.2}$]-(TFE)$_{0.4}$ (**5b**; 3DEMAP$^+$ = 3-(diethyl(methyl)ammonio)phenolate), with quaternization degrees of 87% and 77%, respectively (Scheme 2).

The ^{31}P-NMR spectra of the cationic fluorinated copolyphosphazenes **5a** and **5b** displayed a signal pattern analogous to that of the precursor copolyphosphazenes **4a** and **4b**, with a noticeable shift to higher chemical shifts due to the quaternization of the 3DEAP side groups (Figures S8 and S9, Supporting Information). A similar effect was observed in the ^{1}H-NMR spectra for the methylene and methyl protons of the quaternized 3DEMAP$^+$ groups (Figures S10 and S11, Supporting Information). This downfield shift has been previously reported in other cationic polyphosphazenes bearing —NR$_4^+$ pendant groups.[35,57,58] By integrating the relative signals in the ^{1}H-NMR spectra of **5a** and **5b**, the degree of quaternization was calculated to be 87% for **5a** and 77% for **5b**, resulting in the idealized molecular formulas shown in Scheme 2. As previously mentioned, the ATR-FTIR spectra of the cationic copolymers **5a** and **5b** showed a shift in the C—N stretching signal from 1245 to 1225 cm^{-1} following the formation of the diethylmethylammonium cation. Meanwhile, the P—N backbone stretching modes remained unchanged at ≈1167 and 1268 cm^{-1}, confirming the integrity of the phosphorus-nitrogen backbone during the methylation process (Figures S12 and S13, Supporting Information). This observation is particularly significant because the macromolecular stability and potential main chain degradation during the methylation procedure could not be assessed using GPC measurements. This limitation arose due to the strong interactions between these cationic polyphosphazenes and the column resin, which prevented their elution. Similar effects have been reported for other cationic polyphosphazenes.[35,57,58]

The thermal stability of the as-prepared cationic fluorinated copolyphosphazenes is significantly reduced due to the presence of diethylmethylammonium cation side groups. The TGA/DTG curves of the cationic copolyphosphazenes 5a and 5b (**Figure 3**) revealed onset decomposition temperatures of ≈150 °C, much lower than those of their non-ionic precursors 4a and 4b (≈400 °C). This is primarily attributed to the lower thermal stability of the diethylmethylammonium cations with respect to the non-ionic counterparts. In both thermograms, the DTG curve shows an initial mass loss at ≈150 °C, assigned to the decomposition of the diethylmethylammonium cations (T_{3DEMAP^+}). Following this initial loss, the DTG curve of copolymer 5a (Figure 3a) displayed a mass loss associated with the remaining organic groups (3DEAP and TFE) in the temperature range of 180–420 °C (T_1). In contrast, the thermogram of 5b (Figure 3b) showed two distinct events: one at ≈200 °C for the degradation of trifluoroethoxy groups (T_{TFE}) and another in the range of 280–400 °C for the non-ionic 3DEAP moieties (T_{3DEAP}). The final event above 400 °C in both thermograms corresponds to the thermal degradation of the polymer backbone (T_2), whose stability remains unaffected by the methylation reaction.

The DSC thermograms of the cationic fluorinated copolyphosphazenes **5a** and **5b** exhibited a less pronounced change compared to their non-ionic counterparts **4a** and **4b** (Figure 3c), which can be assigned to their glass transition temperature (T_g). Interestingly, the T_g values for the cationic copolyphosphazenes **5a** (−24 °C) and **5b** (−21 °C) were lower than those of the non-ionic

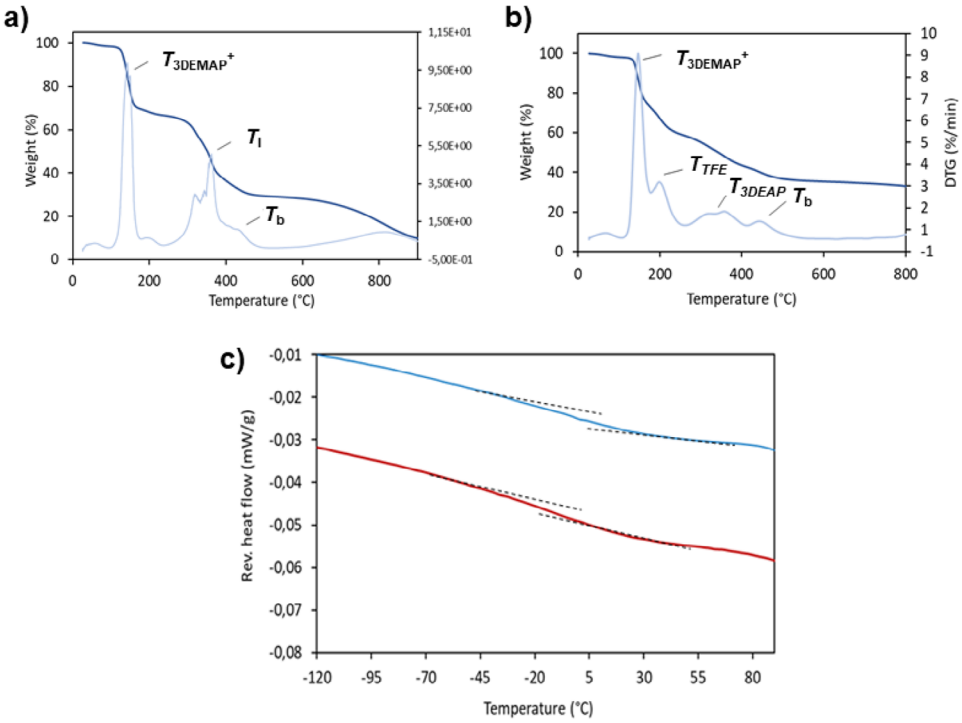

Figure 3. TGA (dark blue) and DTG (light blue) curves of cationic fluorinated copolyphosphazenes: a) [PPz]-[(3DEAP)$_{0.1}$(3DEMAP$^+$)$_{0.9}$]-(TFE)$_{1.0}$ (**5a**) and b) [PPz]-[(3DEAP)$_{0.4}$(3DEMAP$^+$)$_{1.2}$]-(TFE)$_{0.4}$ (**5b**). c) DSC thermograms of cationic fluorinated copolyphosphazenes **5a** (blue) and **5b** (red).

precursors **4a** (−6 °C) and **4b** (10 °C). This trend contrasts with the expected behavior, as ionic moieties typically create interchain associations and reduce chain mobility, leading to higher T_g values. We attribute this anomaly to the random nature of macromolecular substitution in polyphosphazenes and the incomplete quaternization process, which may introduce structural disorder into the copolymers, thereby reducing their overall rigidity.

Table 1. DLS and SLS analysis of aqueous solutions of copolyphosphazenes **5a** and **5b** at 0.33 mg mL^{-1}.

Entry	PPz	$R_{h,App}$ 24 h [nm]	$R_{h,App}$ 72 h [nm]	$R_{g,App}$ [nm]	$R_{g,App}/R_{h,App}$
1	**5a**	58 ± 2	62 ± 1	44 ± 2	0.76 ± 0.04
2	**5b**	724 ± 6	732 ± 4	869 ± 4	1.2 ± 0.07

2.3. Self-Assembly of Cationic Fluorinated Copolyphosphazenes 5a and 5b in Water

The self-assembly of random copolymers in selective solvents to form well-defined nanostructures has been significantly less explored compared to their block copolymer counterparts.[59,60] This difference arises because the self-assembly of block copolymers can typically be precisely controlled and even predicted based on molecular parameters, such as molecular weight, block length, and the chemical nature of each block.[61–66] In contrast, random copolymers often exhibit less defined properties and broader dispersity, making their behavior more challenging to predict. Despite these challenges, random copolymers can still form micelles in selective solvents and microphase-separated domains in thin films.[59,67–70] However, this requires a significantly higher degree of incompatibility between segments and/or a greater solvent selectivity due to the close proximity and short domains of the incompatible repeat units. When these conditions are met, random copolymers can exhibit an even broader range of micelle morphologies (e.g., spheres, rods, honeycombs, vesicles, etc.) compared to block copolymers counterparts.[59,60] Given the high incompatibility between the fluorinated TFE side groups (strongly hydrophobic) and the cationic ammonium substituents (strongly hydrophilic) in the as-prepared copolyphosphazenes **5a** and **5b**, we investigated the self-assembly of these materials in water.

The self-assembly of cationic fluorinated random copolyphosphazenes **5a** and **5b**, featuring different ratios of hydrophobic TFE and hydrophilic quaternized 3DEMAP$^+$ side groups (≈1:1 for **5a** and 1:3 for **5b**), was investigated in water at a concentration of 0.33 mg mL^{-1} using dynamic and static light scattering (DLS and SLS), and transmission electron microscopy (TEM). For this study, precise amounts of copolymers **5a** and **5b** were weighed and dissolved in water via sonication for 2 min using a conventional ultrasonic cleaning bath operating at 35 kHz and 160 W (see Experimental Section). The resulting solutions were periodically monitored by DLS until the apparent hydrodynamic radius ($R_{h,App}$) of the aggregates stabilized, which occurred in both samples after aging at room temperature for 24 h (see **Figure 4a** and **Table 1**). To confirm the stability of the self-assembled structures, the samples were also analyzed after 3 days at room temperature. No significant differences were observed by DLS between

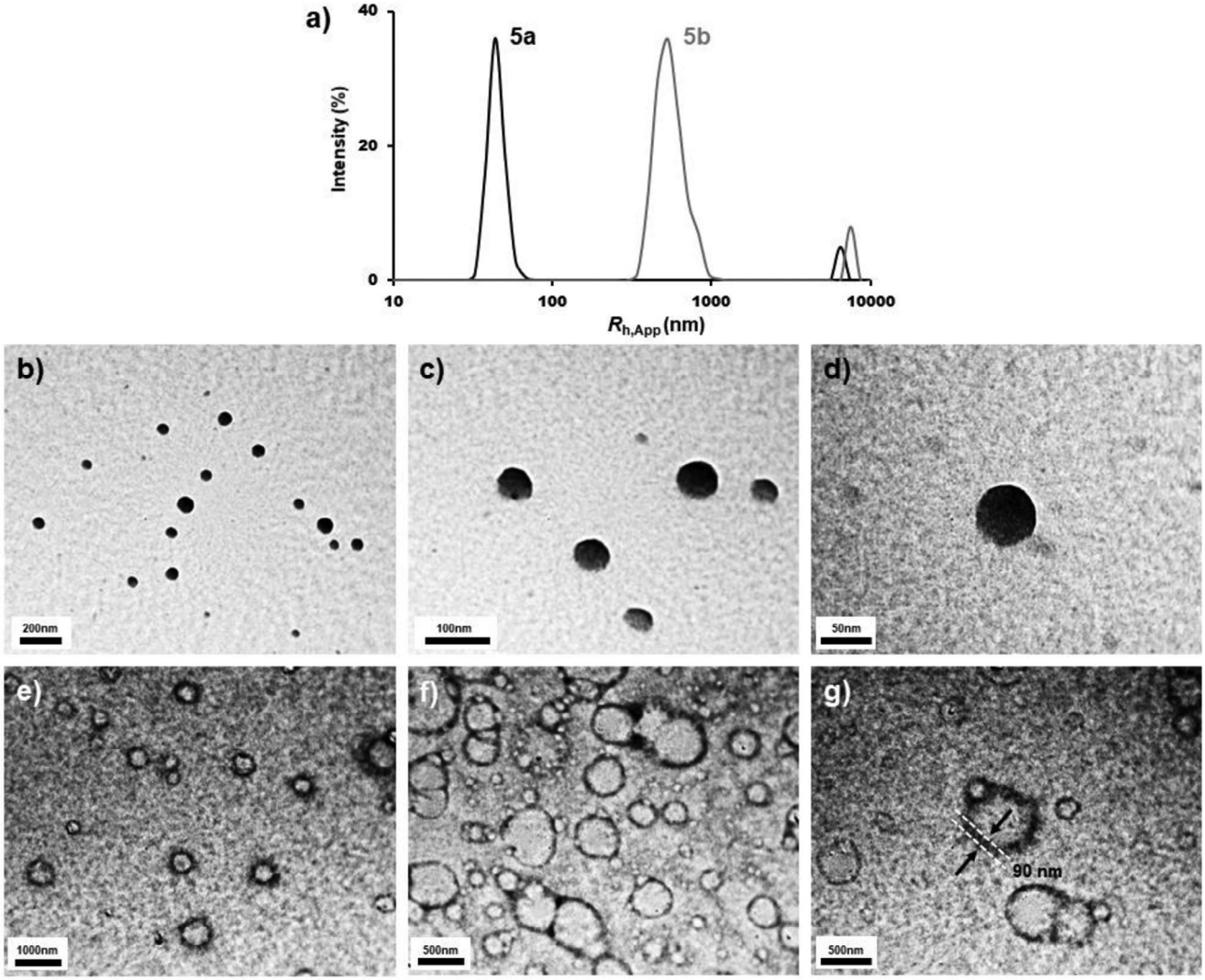

Figure 4. a) Dynamic light scattering (DLS) analysis of 0.33 mg mL^{-1} aqueous solutions of cationic fluorinated copolyphosphazenes **5a** and **5b** after aging for 24 h at 20 °C. b–d) Bright-field TEM images of large compound micelles (LCMs) formed from copolyphosphazene **5a** in water (0.33 mg mL^{-1}). e–g) Bright-field TEM images of vesicles formed from copolyphosphazene **5b** in water (0.33 mg mL^{-1}). Black arrows in (g) indicate the capsule wall of vesicles.

the freshly prepared solutions and those aged for 3 days, indicating that the self-assembly process is effectively complete within the first 24 h of aging. Additionally, the critical micelle concentration (CMC) of both copolymers was estimated as 0.005 mg mL^{-1} based on DLS measurements at varying copolymer concentrations.

TEM analysis of the **5a** solution revealed a single population of particles with a nearly monodisperse spherical morphology. The number-average diameter (D_n) was determined to be 68 nm, with a dispersity (D_w/D_n) of 1.23, both calculated from TEM images (see Experimental Section for details). The 2D projections of these particles are consistent with large compound micelles (LCMs, Figure 4b–d). The nature and internal structure of these aggregates were further inferred from the $R_{g,App}/R_{h,App}$ ratio. The apparent radius of gyration ($R_{g,App}$) was measured as 44 ± 2 nm, yielding an $R_{g,App}/R_{h,App}$ ratio of 0.76 ± 0.04 (entry 1, Table 1). This value is close to the theoretical ratio for solid spheres (0.775)[71,72] and significantly differs from those characteristics of vesicles (1.0) or disk-like morphologies (1.5),[71–74] ruling out the presence of such structures. In contrast, TEM analysis of the **5b** solution, which has a higher proportion of hydrophilic quaternized 3DEMAP$^+$ side groups, revealed the presence of vesicles. These vesicles exhibited a very regular spherical shape but a broad size distribution, with an average diameter (D_n) of 585 nm and a dispersity (D_w/D_n) of 1.8 (Figure 4e–g). The 2D TEM projections of these vesicles showed a darker outer halo, corresponding to the capsule wall, and a lighter interior. Based on the relative solubility of the TFE and 3DEMAP$^+$ side groups, it is expected that TFE-rich clusters form the vesicle wall, while the more hydrophilic 3DEMAP$^+$ domains, with greater affinity for water, are located in the inner and outer coronas. The capsule wall thickness, as determined by TEM, was ≈90 nm. The observation of collapsed and coalescent structures, along with a calculated $R_{g,App}/R_{h,App}$ ratio of 1.2 ($R_{g,App}$ = 869 ± 4 nm; entry 2, Table 1), which is close to the

characteristic value of 1.0 for vesicles, confirms the hollow nature of these nanostructures.

2.4. Decontamination of Anionic Pollutants from Wastewater: Insights from Binding NMR Experiments

Given the high water solubility demonstrated by the cationic fluorinated copolyphosphazenes **5a** and **5b**, and the remarkable biocompatibility of analogous copolyphosphazenes bearing ammonium cationic groups and TFE side groups, we infer that **5a** and **5b** will pose no harm to the environment. As such, they represent promising candidates for pollutant capture in wastewater treatment. Thus, the ability of cationic fluorinated copolyphosphazenes **5a** and **5b** to form insoluble ionic complexes with two common anionic pollutants found in wastewater, sodium diclofenac (SDF) and perfluorooctanoic acid (PFOA), was investigated using binding NMR experiments. First, the capture capacity of SDF was evaluated through ^{1}H-NMR spectroscopy. Thus, a 4 mg mL^{-1} solution of copolymers **5a** and **5b** in D_2O (1 mL) was prepared, and successive aliquots of 30 µL from a 20 mg mL^{-1} D_2O solution of SDF were added (see Table S1, Supporting Information). The chemical shifts of **5a** (**Figure** 5a, spectrum A; SDF = 0 µmol), **5b** (Figure 5b, spectrum A´; SDF = 0 µmol), and SDF (Figure S14, Supporting Information) were used as references. The aromatic proton signal of SDF at 6.4 ppm was selected as it appears in a clear region of the spectra, distinct from the signals of copolymers **5a** and **5b**. The ^{1}H-NMR spectra of successive SDF additions to the aqueous (D_2O) solutions of copolymers **5a** and **5b** are shown in Figure 5a,b, respectively. For cationic copolymer **5a** (CF_3/3DEMAP$^+$ ratio ≈1:1), the polymer signals progressively decreased in intensity with each SDF addition (Figure 5a). This is attributed to the gradual precipitation of the ionic complex formed between cationic copolymer **5a** and SDF, where SDF acts as a counterion instead of iodide (see Figure S15, Supporting Information). SDF signals were not detectable until the addition of 9.45 µmol of the drug, indicating that below a concentration of 2.60 mg mL^{-1} (Table S1, Supporting Information), copolymer **5a** can effectively "capture" and remove SDF from the aqueous solution via precipitation. A similar behavior was observed for cationic copolymer **5b** (CF_3/3DEMAP$^+$ ratio = 1:3). Below a concentration of 2.14 mg mL^{-1}, no SDF signals were detected in the ^{1}H-NMR spectra of successive drug additions (Figure 5b; Table S1, Supporting Information), demonstrating its ability to capture and precipitate SDF below this threshold concentration (see Figure S16, Supporting Information). The lower SDF capture capacity of cationic polyphosphazene **5b** compared to **5a**, despite its higher CF_3/3DEMAP$^+$ ratio (1:3 vs 1:1), can be attributed to several factors including: *i)* the formation of bilayer vesicles by **5b**, where a portion of the 3DEMAP$^+$ groups are located in the inner corona of the vesicles, making them less accessible to SDF (note that the diffusion of hydrophilic SDF molecules through the hydrophobic TFE-rich capsule wall is unlikely); *ii)* on an equal weight basis, the molar amounts of 3DEMAP$^+$ groups in copolyphosphazenes **5a** and **5b** are 4.0 and 3.4 µmol, respectively; and *iii)* the CF_3/3DEMAP$^+$ ratio in **5a** is ≈1:1 which ensures a highly homogeneous distribution of cationic 3DEMAP$^+$ groups along the polymer chains. This prevents the formation of macromolecular regions rich in cationic side groups, which, upon interaction with SDF, could lead to insolubility clusters and the precipitation of the polymeric complexes carrying free 3DEMAP$^+$ groups, as might occur in the case of cationic polyphosphazene **5b**. Importantly, the trapping ability of cationic polyphosphazenes **5a** and **5b** exceeds a 1:1 molar ratio between 3DEMAP$^+$ and SDF, capturing nearly double the molar amount of the drug per cationic site. This behavior suggests that the capture mechanism is not solely based on ionic interactions between the polymer and the drug but also involves hydrophobic interactions with the hybrid hydrophobic/hydrophilic structure of the polymers, which may further enhance the process.

The capture of perfluorooctanoic acid (PFOA) by the cationic copolyphosphazenes **5a** and **5b** was also evaluated using ^{19}F-NMR spectroscopy for this purpose. To this end, 4 mg of each cationic polymer (**5a** and **5b**) were directly added to a 5.5 mg mL^{-1} solution of PFOA in D_2O. The resulting ^{19}F-NMR spectra before (blue) and after (red) the addition are shown in **Figure 6**.

To perform a quantitative analysis without an internal standard, which could potentially interact with the polymer and affect its trapping ability, all spectra were acquired under the same parameters and experimental conditions. Specifically, a relaxation delay (D1) of 10 s, 64 scans (ns), and a receiver gain (RG) of 203 were used. The PFOA signal at −80.9 ppm served as the reference, and its integral was measured in all spectra (Table S2, Supporting Information). The addition of cationic copolyphosphazenes **5a** and **5b** resulted in the formation of precipitates in both cases, due to the formation of insoluble complexes between the cationic polymers and the PFOA molecules. This precipitation process was accompanied by a subsequent decrease in the relative integral of the PFOA reference signal (−80.9 ppm), indicating that a capture process by the cationic copolymers was taking place. Additionally, in both cases, a residual signal at −75 ppm corresponding to the —CF_3 groups of copolyphosphazenes **5a** and **5b** was observed (Figure 6). Nevertheless, based on the relative integration of the signals, almost quantitative water decontamination by cationic copolyphosphazene **5b** was observed, with a removal efficiency of 96.0% (**Table 2**). These efficiencies are comparable to those achieved using polystyrene-based fluorinated ionic polymer gels for the removal of perfluoroalkyl contaminants from water.[75] For polymer **5b**, the weighted amount of PFOA captured corresponded to 13.3 µmol, which is 3.9 times higher than the number of cationic sites on the polymer (3.4 µmol). This promising capture behavior was not observed, however, for cationic **5a**, which has a lower CF_3/3DEMAP$^+$ ratio than that of **5b**. In fact, the binding experiment conducted under the same experimental conditions showed a PFOA removal efficiency of 21.9% (≈5 times lower than that achieved by **5b**), corresponding to 2.9 µmol of removed pollutants, which is lower than the number of available cationic sites on the polymer (Table 2). The amphiphilic nature of both the copolymers and PFOA, derived from the presence of fluorinated (hydrophobic) and ionic (hydrophilic) groups, makes the ionic/hydrophobic interactions between them difficult to predict. In any case, based on the results obtained from the binding experiments, the ionic 3DEMAP$^+$/PFOA interactions, more evident in copolyphosphazene **5b**, appear to prevail over the hydrophobic CF_3/PFOA interactions, which are more numerous in **5a**.

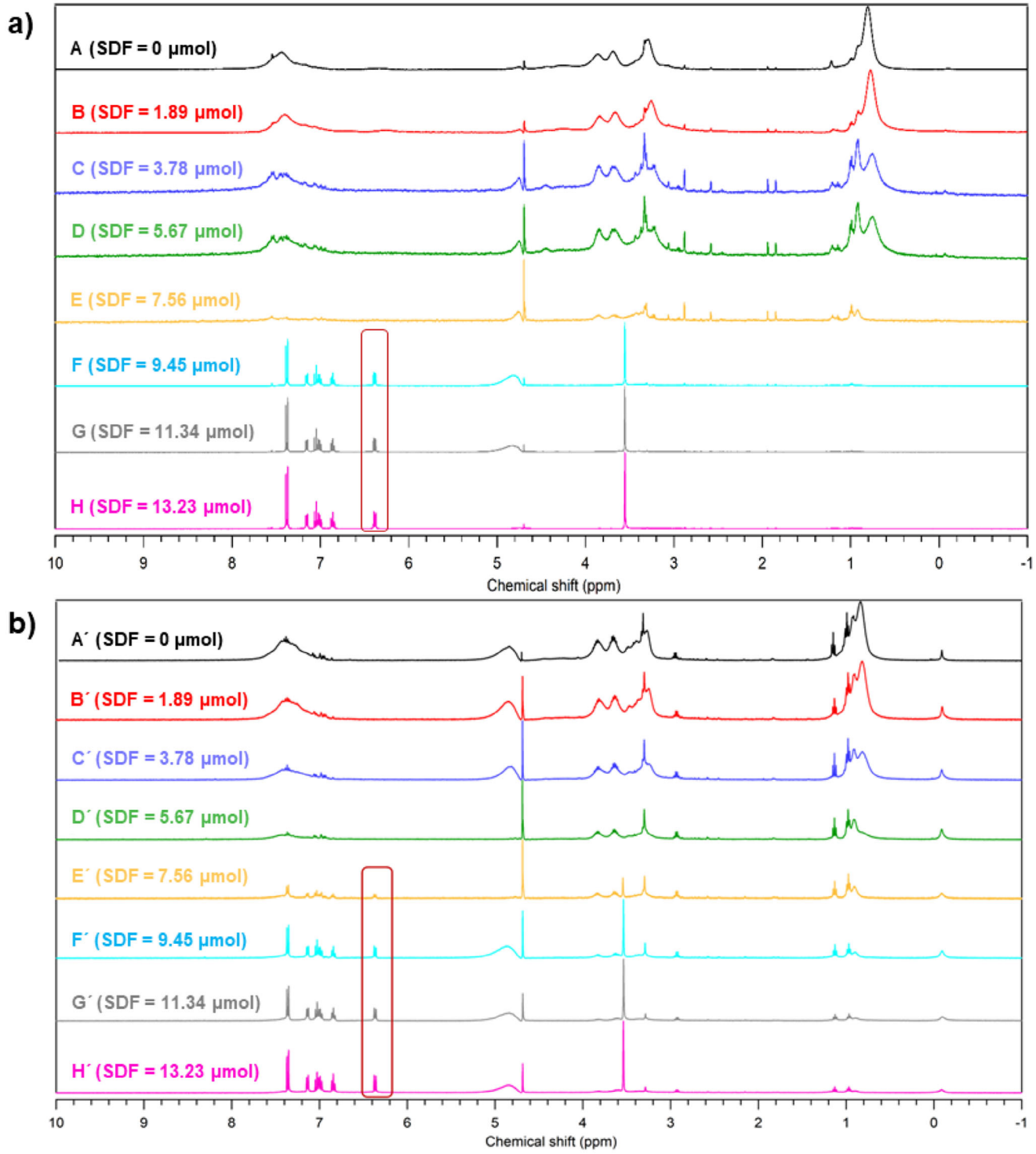

Figure 5. ^{1}H-NMR spectra of successive additions of sodium diclofenac (SDF) to solutions of cationic fluorinated copolyphosphazenes a) **5a** and b) **5b** in D_2O.

3. Conclusion

This work presents a straightforward and efficient methodology for synthesizing well-defined fluorinated copolyphosphazenes with randomly distributed 2,2,2-trifluoroethan-1-olate (–OCH_2CF_3, TFE) and 3-(diethylamino)phenolate (3DEAP) side groups via living cationic polymerization. Mild quaternization of the diethylamino groups with methyl iodide (CH_3I) produced cationic fluorinated copolyphosphazenes with tunable CF_3/3DEMAP$^+$ ratios, exhibiting complete wa-

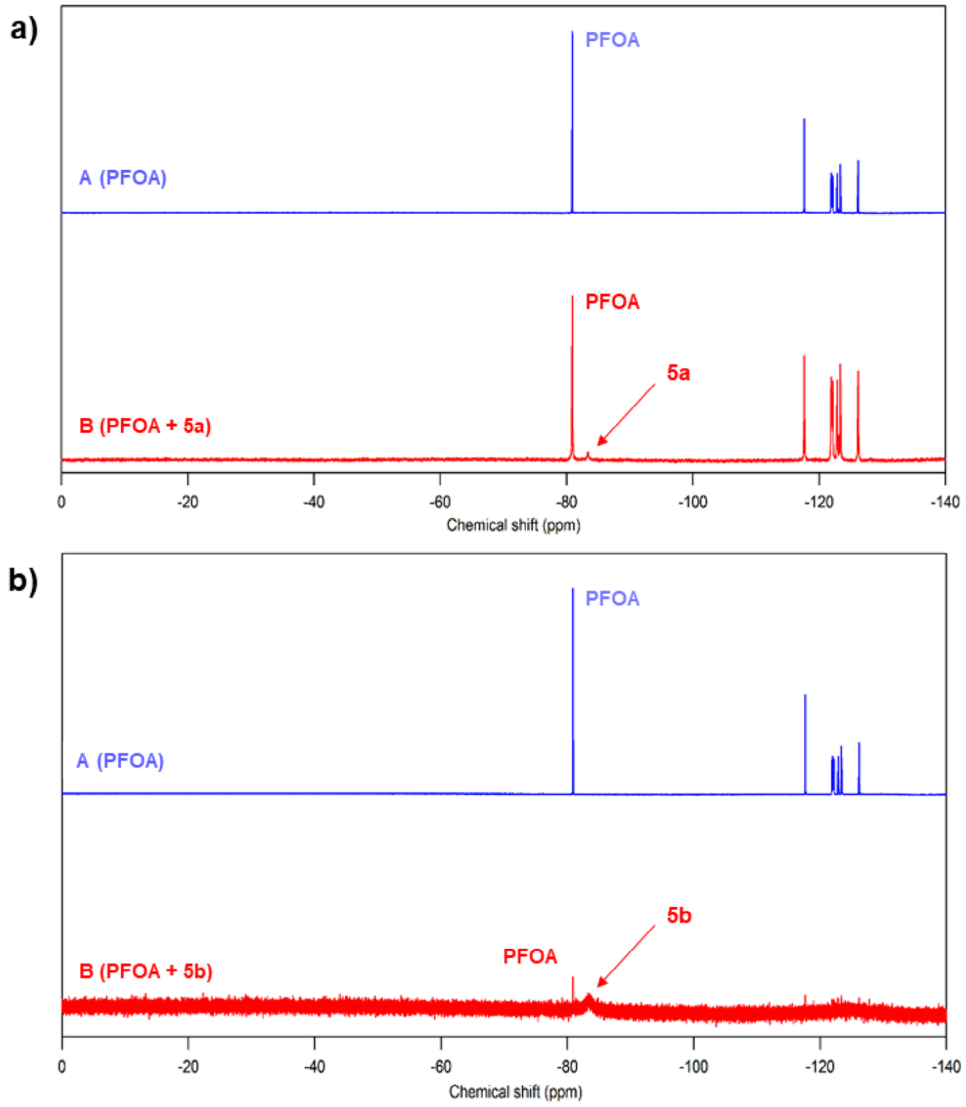

Figure 6. ^{1}H-NMR spectra of addition of cationic fluorinated copolyphosphazenes a) **5a** and b) **5b** to solutions of perfluorooctanoic acid (PFOA) in D_2O.

Table 2. PFOA binding test NMR experiments of cationic copolyphosphazenes **5a** and **5b**.

Entry	PPz[a)]	PFOA Initial Concentration [mg mL^{-1}]	PFOA Final Concentration [mg mL^{-1}]	Removal Efficiency [%]
1	**5a**	5.50	4.29	21.9
2	**5b**	5.50	0.224	96.0

[a)] PPz initial concentration = 4 mg mL^{-1}

ter solubility. These copolymers, combining hydrophobic (CF_3) and hydrophilic (3DEMAP$^+$) moieties, demonstrated self-assembly in aqueous solutions, forming large compound micelles (LCMs) or bilayer vesicles depending on the CF_3/3DEMAP$^+$ ratio. The cationic nature of these materials was effectively employed for the efficient capture of anionic pollutants, such as sodium diclofenac (SDF) and perfluorooctanoic acid (PFOA), which are commonly found in wastewater. This study highlights the potential of these copolyphosphazenes as promising candidates for water decontamination applications.

4. Experimental Section

Materials: All solvents were purchased from Merck. Tetrahydrofuran (THF) and diethyl ether (C_2H_5O) were used after distillation over

sodium and benzophenone, and dichloromethane (CH_2Cl_2) was used after distillation over calcium hydride. Isopropanol (Merck) and methanol (Aldrich) were used as received. PCl_5 was purified by sublimation under reduced pressure and stored under dry N_2 (g). Phosphorus trichloride (PCl_3) and sulfuryl chloride (SO_2Cl_2) were used after distillation under vacuum. 3-diethylaminophenol and 2,2,2-trifluoroethanol, iodomethane (CH_3I), acetonitrile, chloroform, hexane, lithium bis(trimethylsilyl)amide ($LiN(Si(CH_3)_3)_2$), sodium hydride (NaH), sodium diclofenac and perfluorooctanoic acid (PFOA) were used as received, without further purification.

The $Cl_3P{=}N{-}SiMe_3$ (**1**) was synthesized following literature procedures.[76] Freshly distilled PCl_3 (9.36 mL, 0.107 mol) was added dropwise to a solution of $LiN(SiMe_3)_2$ (17.9 g, 0.107 mol) in dry Et_2O (220 mL) at 0 °C. The reaction mixture was stirred for 1 h at room temperature, after which freshly distilled sulfuryl chloride (SO_2Cl_2, 8.65 mL, 0.107 mol) was added dropwise at 0 °C. The reaction was allowed to proceed for 30 min at 0 °C, followed by an additional 1 h at room temperature. The mixture was then filtered through a 1 cm layer of dry Celite (pre-dried overnight at 140 °C). The volatiles were removed from the pale-yellow filtrate by distillation under reduced pressure (Et_2O at 100 mmHg; Cl-$SiMe_3$ at 25 mmHg). The product, $Cl_3P{=}NSiMe_3$, was isolated as a colorless liquid by distilling the remaining residue under a static vacuum (0.1 mmHg), yielding 80%. The synthesized phosphoranimine can be stored under argon at −20°°C and remains stable for several weeks. ^{31}P-NMR ($CDCl_3$, δ ppm) = −58. ^{1}H-NMR ($CDCl_3$, δ ppm) = 0.19; 0.45 (Cl-$SiMe_3$, 2.1% mol).

General Methods: All reactions were carried out under an atmosphere of either dry nitrogen or dry argon using common Schlenk techniques or a glove-box (M-Braun). The purification of the random copolymers by sequential precipitations was performed in the air by dropping a concentrated THF solution of the block copolymer onto a magnetic stirring of pure water, isopropanol or methanol, and/or *n*-hexanes.

Synthesis of poly(dichloro)phosphazene (2): Poly(dichloro)phosphazene ($[N{=}PCl_2]_n$, **2**) was synthesized according to a previously reported procedure by Allcock, Manners, et al.[50,51] Briefly, under strictly inert and anhydrous conditions, 2.5 g (11.13 mmol) of $Cl_3P{=}N{-}SiMe_3$ (**1**) were dissolved in 5 mL of anhydrous dichloromethane (CH_2Cl_2) in a flame-dried Schlenk flask. To this solution, phosphorus pentachloride (PCl_5, 0.8 mol%) was rapidly added under a nitrogen atmosphere. The reaction mixture was stirred at room temperature (20 °C) for 16 h, allowing the polymerization to proceed to completion. After the reaction, the volatiles were removed under reduced pressure, yielding poly(dichloro)phosphazene ($[N{=}PCl_2]_n$, **2**) as a white, viscous oil. The product was used directly in the subsequent reactions without further purification.

2: ^{31}P-NMR (300 MHz, DCM/D_2O as ref) δ (ppm) 7.8 (d, PCl_3^+ end-groups), −14.8 (t, PCl_2PCl_3), −16.0 ppm (t, $PCl_2PCl_2PCl_3$) and −18.2 ppm (br, s,-$(PCl_2)_n$-).

Synthesis of Fluorinated Copolyphosphazenes [PPz]-(3DEPA)$_{1.0}$-(TFE)$_{1.0}$ (4a) and [PPz]-(3DEPA)$_{1.6}$-(TFE)$_{0.4}$ (4b): Both fluorinated copolyphosphazenes, **4a** and **4b**, were synthesized via nucleophilic macromolecular substitution of the previously prepared poly(dichloro)phosphazene (**2**). The synthetic procedure for **4a** and **4b** is described in detail below.

A stirred solution of **2** (1.47 g, 12.65 mmol) in anhydrous tetrahydrofuran (THF, 5 mL) was treated with a THF solution (50 mL) of sodium 3-(diethylamino)phenolate. The sodium 3-(diethylamino)phenolate solution was prepared in situ by reacting 3-diethylaminophenol (2.09 g, 12.65 mmol) with sodium hydride (NaH) 60% dispersion in mineral oil (0.61 g, 15.18 mmol) in THF at 20 °C under an inert atmosphere. The reaction mixture was stirred at room temperature for 6 h, and the progress of the macromolecular substitution was monitored by ^{31}P-NMR spectroscopy. Subsequently, a THF solution (5 mL) of sodium 2,2,2-trifluoroethan-1-olate was added directly to the reaction mixture. The sodium 2,2,2-trifluoroethan-1-olate solution was prepared in situ by reacting 2,2,2-trifluoroethanol (1.77 g, 17.7 mmol) with 60% NaH (0.85 g, 21.24 mmol) in THF at 20 °C. The resulting brown suspension was stirred overnight at room temperature. Completion of the reaction was confirmed by ^{31}P-NMR spectroscopy. The reaction mixture was concentrated using a rotary evaporator, and the residue was precipitated into 1 L of distilled water under vigorous stirring. The polymer was further purified by sequential precipitation from concentrated THF solutions into water and *n*-hexane. The final product was dried at 50 °C under reduced pressure (30 mmHg) for 72 h, yielding **4a** as a solid (83% yield).

4a: ^{31}P-NMR (300 MHz, $CDCl_3$) = δ (ppm) −9.4−−21.2; ^{1}H-NMR (300 MHz, $CDCl_3$) = δ (ppm) 6.0–7.2 (4H, Ar), 3.6–4.4 (2H, CH_2), 2.9–3.4 (4H, CH_2), 0.6–1.3 (6H, CH_3). FT-IR (cm^{-1}): 1268 (PN), 1242 (C—N), 1167 (PN) and 960 (C—F). GPC: M_n = 8.02·10^4, Đ = 1.19. TGA (10 °C min^{-1} under N_2): The polymer was stable until 260 °C. Lost 65.4% of its initial mass in two steps centered at 397 and 470 °C. The final ceramic residue was 34.6% of the initial mass. DSC (10 °C min^{-1} under N_2): T_g = 6 °C. Elemental analysis: C: 44.74%; H: 5.34%; N: 8.86%.

A stirred solution of **2** (1.08 g, 9.32 mmol) in anhydrous tetrahydrofuran (THF, 5 mL) was treated with a THF solution (50 mL) of sodium 3-(diethylamino)phenolate. The sodium 3-(diethylamino)phenolate solution was prepared in situ by reacting 3-diethylaminophenol (2.46 g, 14.91 mmol) with sodium hydride (NaH) 60% dispersion in mineral oil (0.72 g, 17.90 mmol) in THF at 20 °C under an inert atmosphere. The reaction mixture was stirred overnight at room temperature. The progress of the macromolecular substitution was monitored by ^{31}P-NMR spectroscopy. Subsequently, a THF solution (5 mL) of sodium 2,2,2-trifluoroethan-1-olate was added directly to the reaction mixture. The sodium 2,2,2-trifluoroethan-1-olate solution was prepared in situ by reacting 2,2,2-trifluoroethanol (0.65 g, 6.52 mmol) with 60% NaH (0.31 g, 7.82 mmol) in THF at 20 °C. The resulting brown suspension was stirred overnight at room temperature. Completion of the reaction was confirmed by ^{31}P-NMR spectroscopy. The reaction mixture was concentrated using a rotary evaporator, and the residue was precipitated into 1 L of distilled water under vigorous stirring. The polymer was further purified by sequential precipitation from concentrated THF solutions into water and *n*-hexane. The final product was dried at 50 °C under reduced pressure (30 mmHg) for 72 h, yielding **4b** as a solid (79% yield).

4b ^{31}P-NMR (300 MHz, $CDCl_3$) = δ (ppm) −7.8−−27.2; ^{1}H-NMR (300 MHz, $CDCl_3$) = δ (ppm) 6.0–7.2 (4H, Ar), 3.7–4.5 (2H, CH_2), 2.8–3.5 (4H, CH_2), 0.6–1.4 (6H, CH_3). FT-IR (cm^{-1}): 1273(PN), 1250 (C—N), 1170 (PN) and 965 (C—F). GPC: M_n = 8.02·10^4, Đ = 1.21. TGA (10 °C min^{-1} under N_2): The polymer was stable until 140 °C. Lost 55.5% of its initial mass in four steps centred at 253, 317, 378, and 463 °C. The final ceramic residue was 44.5% of the initial mass. DSC (10 °C min^{-1} under N_2): T_g = 10 °C. Elemental analysis: C: 49.54%; H: 5.86%; N: 9.99%.

Synthesis of Cationic Fluorinated Copolyphosphazenes [PPz]-[(3DEPA)$_{0.1}$(3DEMAP$^+$)$_{0.9}$]-(TFE)$_{1.0}$ (5a) and [PPz]-[(3DEPA)$_{0.4}$(3DEMAP$^+$)$_{1.2}$]-(TFE)$_{0.4}$ (5b): Both cationic fluorinated copolyphosphazenes, **5a** and **5b**, were synthesized via methylation reaction with CH_3I of the previously prepared copolyphosphazenes **4a** and **4b**. The synthetic procedure for **5a** and **5b** is described in detail below.

Over a stirred solution of **4a** (0.62 g, 1.77 mmol) in a mixture of $CHCl_3/CH_3CN$ 1:3 (20 mL), methyl iodide (CH_3I) (3.77 g, 26.55 mmol) was added dropwise under continuous stirring and a steady flow of nitrogen. The reaction mixture was maintained at 55 °C for 18 h, and the progress of the reaction was monitored by ^{1}H-NMR spectroscopy. After completion of the reaction, the mixture was concentrated under reduced pressure using a rotary evaporator. The resulting residue was washed twice with diethyl ether. The final product was dried at 50 °C under vacuum (30 mmHg) for 72 h, yielding the cationic fluorinated copolyphosphazene **5a** as a solid (87% yield).

5a: ^{31}P-NMR (300 MHz, CD_3CN) δ (ppm) −8.1−−13, −13−−19; ^{1}H-NMR (300 MHz, $CDCl_3$) = δ (ppm) 6.3–8.0 (4H, Ar), 3.8–4.8 (2H, CH_2; 4H, CH_2), 2.9–3.5 (4H, CH_2), 2.6–2.9 (3H, CH_3), 0.8–1.3 (6H, CH_3). FT-IR (cm^{-1}): 12 650 (C—N), 1274 (PN), 1161 (PN) and 957 (C—F). TGA (10 °C min^{-1} under N_2): The polymer was stable until 120 °C. Lost 90.4% of its initial mass in three steps centered at 143, 360, and 430 °C. The final ceramic residue was 9.6% of the initial mass. DSC (10 °C min^{-1} under N_2): T_g = −24 °C.

Over a stirred solution of **4b** (0.956 g, 3.11 mmol) in a mixture of $CHCl_3/CH_3CN$ 1:3 (25 mL), methyl iodide (CH_3I) (6.621 g, 46.65 mmol) was added dropwise under continuous stirring and a steady flow of nitrogen. The reaction mixture was maintained at 55 °C for 18 h, and the

progress of the reaction was monitored by ^{1}H-NMR spectroscopy. After completion of the reaction, the mixture was concentrated under reduced pressure using a rotary evaporator. The resulting residue was washed twice with diethyl ether. The final product was dried at 50 °C under vacuum (30 mmHg) for 72 h, yielding the cationic fluorinated copolyphosphazene **5a** as a solid (85% yield).

5b ^{31}P-NMR (300 MHz, MeOD) = δ (ppm) −8.6–−25.9; ^{1}H-NMR (300 MHz, MeOD) = δ (ppm) 7.1–8.3 (4H, Ar), 4.4–4.8 (2H, CH_2), 3.8–4.3 (4H, CH_2), 3.6–3.8 (4H, CH_2), 3.4–3.6 (3H, CH_3), 0.9–1.3 (6H, CH_3). FT-IR (cm^{-1}): 1265 (C—N), 1275 (PN), 1165 (PN) and 958 (C—F). TGA (10 °C min^{-1} under N_2): The polymer was stable until 130 °C. Lost 67.2% of its initial mass in four steps centered at 140, 200, 343, and 447 °C. The final ceramic residue was 32.8% of the initial mass. DSC (10 °C min^{-1} under N_2): T_g = −21 °C.

Measurements and Characterization Techniques—Nuclear Magnetic Resonance Spectroscopy (NMR): Monodimensional multinuclear NMR spectra were recorded at 20 °C on Bruker NAV-400, DPX-300, and AV-400 instruments. ^{1}H spectra were given relative to $Si(CH_3)_4$, $^{31}P\{^1H\}$-NMR spectra were given relative to external 85% aqueous H_3PO_4. ^{19}F NMR resonances are given relative to an external reference of CF_3COOH.

Measurements and Characterization Techniques—Attenuated Total Reflectance Fourier Transform Infrared Spectroscopy (ATR-FTIR): The spectra were acquired by attenuated total reflectance Fourier Infrared Spectroscopy (ATR-FTIR) analyses. The spectra were recorded with a Perkin–Elmer Spectrum 100 instrument in the range of 4000–500 cm^{-1}.

Measurements and Characterization Techniques—Elemental Analysis (CHN): Elemental analyses were conducted using a FLASH 2000 CHNS-O Organic Elemental Analysis analyzer. The measurements were performed on the dry polymers. Each sample was analyzed at least three times.

Measurements and Characterization Techniques—Gel Permeation Chromatography (GPC): GPC traces were measured with a Perkin–Elmer equipment with a model LC 250 pump, a model LC 290 UV, and a model LC 30 refractive index detector. The samples were eluted with a 0.1% by weight solution of tetra(*n*-buthyl)ammonium bromide in THF through Perkin–Elmer PLGel (Guard, 10^5, 10^4, and 10^3 Å) at 30 °C. Approximate molecular weight calibration was obtained using narrow molecular weight distribution of polystyrene standards. Samples were typically prepared by dissolving 10 mg of the polymer sample in 10 mL of micro-filtered (Millipore–Millex 0.45 µm) HPLC-grade THF. The mixture was sonicated for 5 min and magnetically stirred during 2 h. An aliquot of the solution was then filtered again (Millipore–Millex 0.45 µm) to remove any insoluble material, and injected (20 µL) to the GPC (1 mL min^{-1}).

Measurements and Characterization Techniques—Thermogravimetric Analysis (TGA): The measurements were performed with thermobalance Mettler TGA/SDTA 851e. The analyses were conducted from 25 °C to 800 °C under nitrogen flow. The heating ramp was 10 °C min^{-1}.

Measurements and Characterization Techniques—Modulated Differential Scanning Calorimetry (MDSC): The Modulated Differential Scanning Calorimetry (MDSC) analysis was carried out using a Q20 instrument (TA Instrument), equipped with a liquid nitrogen cooling system. The measurements were collected in a modulated mode with ± 1.000 °C modulation every 60 s and a heat rate of 3.00 °C min^{-1}. 3–5 mg of samples were loaded inside a hermetically sealed aluminum pan.

Measurements and Characterization Techniques—Transmission Electron Microscope (TEM): Bright field TEM micrographs were obtained on a JEOL JEM-FS2200 HRP microscope operating at 200 kV and equipped with a GATAN digital camera. No staining of the samples was necessary. However, to enhance the contrast, a RuO_4 stain was performed in some of the samples (the stained TEM pictures are indicated in the text or in the caption of each figure). To stain the samples, a water solution of RuO_4 was freshly prepared before every stained process by treatment of 20 mg of $RuCl_3$ with 1 mL of sodium hypochlorite (10% solution in water). The films were stained during 2 h. For the statistical length analysis, nanostructures were traced manually using ImageJ software (http://rsb.info.nih.gov/ij/) to determine the contour length. Each TEM micrograph was analyzed completely (every single micelle in each image) in order to reduce subjectivity. From this data, the number average diameter (D_n) and weight average diameter (D_w) were calculated as shown below (N = number of objects that have been traced and D = diameter of the object).

$$D_n = \frac{\sum_{i=1}^{n} N_i D_i}{\sum_{i=1}^{n} N_i} \quad D_w = \frac{\sum_{i=1}^{n} N_i D_i^2}{\sum_{i=1}^{n} N_i D_i} \tag{1}$$

Measurements and Characterization Techniques—Dynamic and Static Light Scattering Analysis: Dynamic light scattering (DLS) measurements were performed using a Malvern 4700 system equipped with a PCS5101 goniometer, a PCS7 stepper motor controller, a Cyonics Ar^+ laser (690 nm, 10 mW), a PCS8 temperature control unit, and an RR98 pump/filtering unit. Data were collected at a detection angle of 173° (backscattering) and analyzed using the Malvern DTS 5.02 software. Correlation functions were processed using the cumulant method and CONTIN software. Each sample was measured five times, and the results were averaged. Static light scattering (SLS) measurements were conducted on the same instrument, with angles ranging from 30° to 150° in 10° increments. Each sample was measured three times, and the results were averaged. Toluene was used as the calibration standard, and dn/dc values were obtained from the literature.[77] The gyroscopic ratio was calculated using the 2nd-order Guinier mode.

Supporting Information

Supporting Information is available from the Wiley Online Library or from the author.

Acknowledgements

All the authors thank MCIN/AEI/10.13039/501100011033 (project numbers: PID2020-113473GB-100, RED2022-134287-T, PID2023-148663NB-I00), "Programa de Subvenciones para grupos de investigación de organismos del Principado de Asturias" [IDE/2024/000727; ref. SEK-25-GRU-GIC-24-048], P.S. and F.L. thank the UNIPD-DII BIRD2023 project "HYPURE-Hybrid 3D Printed Water Purification Systems for Emerging Pollutants", for financial support. M. Ramos-Martín acknowledges a predoctoral award from "Programa Severo Ochoa para la formación en investigación y docencia del Principado de Asturias" (PA-21-PF-BP20-093).

Conflict of Interest

The authors declare no conflict of interest.

Data Availability Statement

The data that support the findings of this study are available in the supplementary material of this article.

Keywords

cationic polymers, fluoropolymers, polyphosphazene, wastewater decontamination

Received: March 25, 2025
Revised: April 25, 2025
Published online:

[1] G. Farzi, M. Gheysipour, *Principles of Biomaterials Encapsulation : Volume Two*, Elsevier, Amsterdam, Netherlands **2023**, pp. 3–38.

[2] A. G. Fane, R. Wang, M. X. Hu, *Angew Chem Int Ed* **2015**, *54*, 3368.
[3] B. Ameduri, *Encyclopedia of Polymer Science and Technology*, (Ed.: H. F. Mark), Wiley, Hoboken, NJ, USA **2012**.
[4] G. Hougham, P. E. Cassidy, K. Johns, T. Davidson (Eds.), *Fluoropolymers 1: Synthesis*, 1st ed., Springer, New York, NY **2002**.
[5] J. G. Drobny, A. L. Moore, *Fluoroelastomers Handbook: The Definitive User's Guide*, William Andrew, Norwich, NY **2005**.
[6] B. Ameduri, *Chem. Eur J* **2018**, *24*, 18830.
[7] M. G. Dhara, S. Banerjee, *Prog. Polym. Sci.* **2010**, *35*, 1022.
[8] Z. Cui, E. Drioli, Y. M. Lee, *Prog. Polym. Sci.* **2014**, *39*, 164.
[9] B. Améduri, B. Boutevin, G. Kostov, *Prog. Polym. Sci.* **2001**, *26*, 105.
[10] E. T. Kang, Y. Zhang, *Adv. Mater.* **2000**, *12*, 1481.
[11] A. L. Logothetis, *Prog. Polym. Sci.* **1989**, *14*, 251.
[12] H. R. Allcock, *Soft Matter* **2012**, *8*, 7521.
[13] S. Rothemund, I. Teasdale, *Chem. Soc. Rev.* **2016**, *45*, 5200.
[14] H. R. Allcock, C. Chen, *J. Org. Chem.* **2020**, *85*, 14286.
[15] H. R. Allcock, *Dalton Trans.* **2016**, *45*, 1856.
[16] H. R. Allcock, *Chemistry and Applications of Polyphosphazenes* **2002**.
[17] K. A. Andrianov (Ed.), *Polyphosphazenes for Biomedical Applications*, John Wiley & Sons, Hoboken, NJ. USA **2009**.
[18] P. Ilayaperumal, P. Chelladurai, K. Vairan, P. Anilkumar, B. Balagurusamy, *Macromol. Mater. Eng.* **2023**, *308*, 2200553.
[19] F. Chen, O. R. Teniola, C. T. Laurencin, *J. Mater. Res.* **2022**, *37*, 1417.
[20] G. Casella, S. Carlotto, F. Lanero, M. Mozzon, P. Sgarbossa, R. Bertani, *Molecules* **2022**, *27*, 8117.
[21] G.-W. Jin, N. S. Rejinold, J.-H. Choy, *IJMS* **2022**, *23*, 15993.
[22] Z. Ali, M. Basharat, Z. Wu, *ChemElectroChem* **2021**, *8*, 759.
[23] A. K. Andrianov, R. Langer, *J. Controlled Release* **2021**, *329*, 299.
[24] X. Zhou, S. Qiu, X. Mu, M. Zhou, W. Cai, L. Song, W. Xing, Y. Hu, *Compos. B Eng.* **2020**, *202*, 108397.
[25] W. Hsu, N. Csaba, C. Alexander, M. Garcia-Fuentes, *J. Appl. Polym. Sci.* **2020**, *137*, 48688.
[26] G. A. Carriedo, R. De La Campa, A. P. Soto, *Eur. J. Inorg. Chem.* **2018**, *2018*, 2484.
[27] R. S. Ullah, L. Wang, H. Yu, N. M. Abbasi, M. Akram, Z. ul-Abdin, M. Saleem, M. Haroon, R. U. Khan, *RSC Adv.* **2017**, *7*, 23363.
[28] W.-L. Chiu, C.-I. Huang, *Polymers* **2023**, *15*, 3198.
[29] M. Gleria, R. Bertani, R. D. Jaeger, S. Lora, *J. Fluor. Chem.* **2004**, *125*, 329.
[30] M. Gleria, R. Bertani, R. De Jaeger, *J. Inorg. Organomet. Polym.* **2004**, *14*, 1.
[31] V. Albright, A. Marin, P. Kaner, S. A. Sukhishvili, A. K. Andrianov, *ACS Appl. Bio Mater.* **2019**, *2*, 3897.
[32] V. Selin, V. Albright, J. F. Ankner, A. Marin, A. K. Andrianov, S. A. Sukhishvili, *ACS Appl. Mater. Interfaces* **2018**, *10*, 9756.
[33] V. Albright, D. Penarete-Acosta, M. Stack, J. Zheng, A. Marin, H. Hlushko, H. Wang, A. Jayaraman, A. K. Andrianov, S. A. Sukhishvili, *Biomaterials* **2021**, *268*, 120586.
[34] A. K. Andrianov, A. Marin, P. Peterson, J. Chen, *J. Appl. Polym. Sci* **2007**, *103*, 53.
[35] A. Marin, J. Brito, S. A. Sukhishvili, A. K. Andrianov, *ACS Appl. Bio Mater.* **2022**, *5*, 313.
[36] T. Saah, *Harm Reduct. J* **2005**, *2*, 8.
[37] R. C. Buck, J. Franklin, U. Berger, J. M. Conder, I. T. Cousins, P. De Voogt, A. A. Jensen, K. Kannan, S. A. Mabury, S. P. Van Leeuwen, *Integr. Environ. Asses. Manag.* **2011**, *7*, 513.
[38] P. Sathishkumar, K. Mohan, R. A. A. Meena, M. Balasubramanian, L. Chitra, A. R. Ganesan, T. Palvannan, S. K. Brar, F. L. Gu, *J. Hazard. Mater.* **2021**, *419*, 126135.
[39] A. Fahimi, A. Zanoletti, S. Federici, A. Assi, F. Bilo, L. E. Depero, E. Bontempi, *Materials* **2020**, *13*, 3964.
[40] K. A. Barzen-Hanson, S. C. Roberts, S. Choyke, K. Oetjen, A. McAlees, N. Riddell, R. McCrindle, P. L. Ferguson, C. P. Higgins, J. A. Field, *Environ. Sci. Technol.* **2017**, *51*, 2047.
[41] C. V. T. Rigueto, M. Rosseto, M. T. Nazari, B. E. P. Ostwald, I. Alessandretti, C. Manera, J. S. Piccin, A. Dettmer, *J. Environ. Chem. Eng.* **2021**, *9*, 105030.
[42] Y. Long, Y. Feng, X. Li, N. Suo, H. Chen, Z. Wang, Y. Yu, *Chemosphere* **2019**, *219*, 1024.
[43] P. Finkbeiner, M. Franke, F. Anschuetz, A. Ignaszak, M. Stelter, P. Braeutigam, *Chem. Eng. J.* **2015**, *273*, 214.
[44] A. Abilarasu, P. S. Kumar, D.-V. N. Vo, D. Krithika, P. T. Ngueagni, G. J. Joshiba, C. F. Carolin, G. Prasannamedha, *J. Environ. Chem. Eng.* **2021**, *9*, 104875.
[45] J.-H. Hwang, Y. Y. Li Sip, K. T. Kim, G. Han, K. L. Rodriguez, D. W. Fox, S. Afrin, A. Burnstine-Townley, L. Zhai, W. H. Lee, *Chemosphere* **2022**, *296*, 134001.
[46] Z. Ren, U. Bergmann, T. Leiviskä, *Water Res.* **2021**, *205*, 117676.
[47] Q. Luo, S. Liang, Q. Huang, *J. Hazard. Mater.* **2018**, *359*, 241.
[48] L. Yi, Q. Peng, D. Liu, L. Zhou, C. Tang, Y. Zhou, L. Chai, *Environ. Technol.* **2019**, *40*, 3153.
[49] P. Luo, Y. Zhang, Z. Peng, Q. He, W. Zhao, W. Zhang, D. Yin, Y. Zhang, J. Tang, *Environ. Pollut.* **2024**, *343*, 123212.
[50] C. H. Honeyman, I. Manners, C. T. Morrissey, H. R. Allcock, *J. Am. Chem. Soc.* **1995**, *117*, 7035.
[51] H. R. Allcock, C. A. Crane, C. T. Morrissey, J. M. Nelson, S. D. Reeves, C. H. Honeyman, I. Manners, *Macromolecules* **1996**, *29*, 7740.
[52] H. R. Allcock, S. D. Reeves, C. R. De Denus, C. A. Crane, *Macromolecules* **2001**, *34*, 748.
[53] Y. Chen, Z. Li, N. Chen, Y. Zhang, F. Wang, H. Zhu, *Electrochim. Acta* **2017**, *258*, 311.
[54] A. King, D. Presnall, L. B. Steely, H. R. Allcock, K. J. Wynne, *Polymer* **2013**, *54*, 1123.
[55] W. T. Ferrar, A. S. Marshall, J. Whitefield, *Macromolecules* **1987**, *20*, 317.
[56] H. R. Allcock, M. N. Mang, A. A. Dembek, K. J. Wynne, *Macromolecules* **1989**, *22*, 4179.
[57] V. Vajihinejad, S. P. Gumfekar, D. V. Dixon, M. A. Silva, J. B. P. Soares, *Sep. Purif. Technol.* **2021**, *260*, 118183.
[58] V. Vajihinejad, S. P. Gumfekar, B. Bazoubandi, Z. Rostami Najafabadi, J. B. P. Soares, *Macromol. Mater. Eng.* **2019**, *304*, 1800526.
[59] L. Li, K. Raghupathi, C. Song, P. Prasad, S. Thayumanavan, *Chem. Commun.* **2014**, *50*, 13417.
[60] I. Sadeghi, A. Asatekin, *Macromol. Chem. Phys.* **2017**, *218*, 1700226.
[61] J. K. Kim, S. Y. Yang, Y. Lee, Y. Kim, *Prog. Polym. Sci.* **2010**, *35*, 1325.
[62] Q. Zhang, N. R.e Ko, J. K. Oh, *Chem. Commun.* **2012**, *48*, 7542.
[63] Z. Ge, S. Liu, *Chem. Soc. Rev.* **2013**, *42*, 7289.
[64] A.-V. Ruzette, L. Leibler, *Nature Mater* **2005**, *4*, 19.
[65] H.-C. Kim, S.-M. Park, W. D. Hinsberg, *Chem. Rev.* **2010**, *110*, 146.
[66] Y. Mai, A. Eisenberg, *Chem. Soc. Rev.* **2012**, *41*, 5969.
[67] X. Zhu, M. Liu, *Langmuir* **2011**, *27*, 12844.
[68] R. Cheng, M. Tian, S. Sun, C. Liu, Y. Wang, Z. Liu, Z. Liu, J. Jiang, *Langmuir* **2015**, *31*, 7758.
[69] P. Bengani, Y. Kou, A. Asatekin, *J. Membr. Sci.* **2015**, *493*, 755.
[70] P. Bengani-Lutz, E. Converse, P. Cebe, A. Asatekin, *ACS Appl. Mater. Interfaces* **2017**, *9*, 20859.
[71] W. Burchard, *Light Scattering from Polymers*, Springer, Berlin Heidelberg **1983**, pp. 1–124.

[72] M. B. Huglin, *Light Scattering from Polymer Solution*, Academic Press, London, New York **1972**.
[73] J. Wu, E. M. Pearce, T. K. Kwei, A. A. Lefebvre, N. P. Balsara, *Macromolecules* **2002**, *35*, 1791.
[74] S. Zhou, C. Burger, B. Chu, M. Sawamura, N. Nagahama, M. Toganoh, U. E. Hackler, H. Isobe, E. Nakamura, *Science* **2001**, *291*, 1944.
[75] S. P. Sahu, O. T. Adeleye, S. Antwi, F. Donnarumma, N. Nidamanuri, R. Bhise, E. Gadekar, S. Sharma, R. Srivastava, Y. Wang, *React. Funct. Polym.* **2025**, *207*, 106138.
[76] B. Wang, E. Rivard, I. Manners, *Inorg. Chem.* **2002**, *41*, 1690.
[77] J. Brandrup, E. H. Immergut, (Ed.: E. A. Grulke), *Polymer Handbook*, 4th ed., Wiley, New York, USA **1999**.